

## TWO NOVEL TECHNIQUES OF TRITIUM MEASUREMENT AT THE FUSION NEUTRONICS FACILITY LOTUS

A. Kumar<sup>@</sup>, S. Azam, W. Leo<sup>+</sup>, Ch. Sahraoui, P. Strasser, F. Fernandez, and J.-P. Schneeberger

Institut de Génie Atomique, Ecole Polytechnique Fédérale de Lausanne, CH-1015 Lausanne,  
Switzerland

<sup>@</sup> Present Address : M.A.N.E.D., UCLA, Los Angeles, CA 90024, USA

<sup>+</sup> Present Address : O.F.A.C. - Geneva - Switzerland

**Abstract** : The tritium measurement in deep locations of a fusion blanket by the conventional techniques, based on liquid scintillation and thermoluminescent dosimetry, is subject to limitation because of their low sensitivity, the low neutron flux and the constraint of limited operation time of the D-T neutron generator. Two novel techniques have been developed and tested at the LOTUS facility, based on : (i) Lithium Glass Scintillation (LGS), and (ii) Solid State Nuclear Track Detection (SSNTD). The LGS has been conventionally used for the measurement of low-energy flux because of  $1/v$  cross-section behaviour of  ${}^6\text{Li}(n,\alpha)t$  reaction. The lithium glass scintillator (NE912 or NE913) used in the present experiment is only 1mm thick. For the SSNTD method, we have used  ${}^6\text{Li}$  and  ${}^7\text{Li}$  enriched 2 mm thick LiF foils as the source for the commercially available LR115 type II detector. A benchmark experimental assembly consisting of 10 cm thick Pb followed by 22 cm thick  $\text{Li}_2\text{CO}_3$  slabs was irradiated by 14 MeV neutrons. The tritium production rates (TPR) were measured at a number of axial locations. The comparison of normalized spatial profiles shows that the two techniques give matching result. However, both the profiles have significant discrepancies with the computed profile by a 2D code. The SSNTD technique also yields the profile for TPR from  ${}^7\text{Li}(n,n'\alpha)t$  that is close to the one from the 2D code.

[tritium measurement, lithium glass scintillator, solid state nuclear track detector, benchmark experiment]

### Introduction

The fusion blankets are optimized with a tritium breeding ratio (TBR) of more than 1. It is important to make sure that the neutron cross-section data used in a design calculation is accurate enough so as to have good confidence in the viability of the design<sup>1</sup>. There have been a number of measurements on simplified blanket models<sup>1-5</sup>. Some of them have found discrepancies in the measured and the calculated TBRs. It is to be pointed out that the conventionally used tritium measuring methods, liquid scintillation<sup>5</sup> and thermoluminescent dosimetry, have poor performance in the deeper regions of a blanket, because of low statistics, where the discrepancies in the nuclear cross-section data are expected to manifest themselves. Thus, it is crucial to develop more sensitive tritium measuring techniques. We have worked, at the LOTUS facility, on developing two novel techniques which are based on (i) Lithium Glass Scintillation (LGS) and (ii) Solid State Nuclear Track Detection (SSNTD). The LGS is inspired by the already existing use of  ${}^6\text{Li}$  enriched lithium glass as low-energy neutron detector. Of late, it was applied to TBR in a fusion blanket<sup>6</sup>. Our technique is a little different than the one reported in the reference (6). The SSNTD is still being very actively pursued with many ameliorations in the track counting methods<sup>7</sup>. The advent of image analyzers has improved the accuracy and the efficiency of track-counting. With this background in mind, the first feasibility tests were carried out successfully in 1986 at our facility and it was decided to continue to develop this method further<sup>8</sup>. The benchmark experiment together with the results are presented and discussed.

### Lithium Glass Scintillation Technique

Two types of lithium glass were selected: NE912 (95%  ${}^6\text{Li}$ ) and NE913 (99.99%  ${}^7\text{Li}$  + 0.01%  ${}^6\text{Li}$ ). NE912 responds to neutrons,  $\gamma$ 's and electrons due to the  $1/v$  dependence of  ${}^6\text{Li}(n,\alpha)t$  cross-section on energy and

its exothermic character. NE913, devoid of  ${}^6\text{Li}$ , has much reduced response to low-energy neutrons and is as responsive to  $\gamma$ 's and electrons as NE912. The pulse shape and pulse height discrimination is used to take out  $\gamma$  component in the experiments. To first-order approximation, it could be said that NE913 is suitable to measure the background to the contribution of low-energy neutrons in NE912.

### Background Reactions

The composition of the lithium glasses, given by the manufacturer, is as follows: 75 wt%  $\text{SiO}_2$ , 21 wt%  $\text{Li}_2\text{O}$ , 4 wt%  $\text{Ce}_2\text{O}_3$ . Each scintillator weighs 200 mg and is 1 mm thick with a diameter of 10 mm. The active volume of the detector is only  $0.08 \text{ cm}^3$  [1/3 of the active volume of the LGS in reference (6)]. Thus, NE912 is expected to provide interesting spatial resolution, little flux perturbation and negligible self-shielding effect. Table 1 shows 2-D calculated contributions of different neutron-induced reactions in both the lithium glasses in a quite soft neutron spectrum location.

**Table 1**  
Relative Contribution of Different Reactions in LGS

Reaction	In the NE912	In the Background	
		NE912	NE913
${}^6\text{Li}(n,\alpha)t$	86.3%	-	-
${}^6\text{Li}(n,n'd)\alpha$	5.0%	36.5%	0.0%
${}^6\text{Li}(n,p)$	0.1%	0.7%	0.0%
Si(net)	5.1%	37.2%	45.6%
O(net)	3.4%	24.8%	29.9%
${}^7\text{Li}(n,n't)\alpha$	0.1%	0.8%	24.0%

All the consequential reactions resulting in charged particle production have been included. The contributory reactions have been summed up for Si and O and are labelled by 'net' in the table. It is seen that the contributions of different reactions are not

the same for both the scintillators even in Si and O. The background in NE912 - the sum of all other reactions than  ${}^6\text{Li}(n,\alpha)t$  - is 13.7%. For other neutron spectrum, the difference in the two background data might be even larger as the threshold parasitic reactions in  ${}^6\text{Li}$  are expected to go up further at the expense of  ${}^6\text{Li}(n,\alpha)t$ . The  $\gamma$ -contributions, not considered in the table 1, to the scintillator responses would not be identical (they would be affected differently under harder neutron spectrum). Thus the use of NE913 as an estimator of the background is not self-evident. We have, therefore, worked on two different methods of data-treatment as discussed later.

### Detector Set-up

Figure. 1. shows the block-diagram of the pulse shape discrimination circuitry while the LGS detector

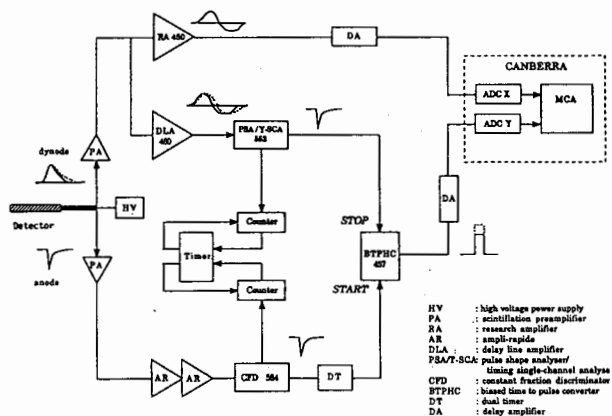


Figure 1: Block-Diagram of the Electronic Circuit

assembly is shown in Figure 2. This circuit allows to collect the counts as a function of both the pulse height and pulse shape. 128 channels were provided.

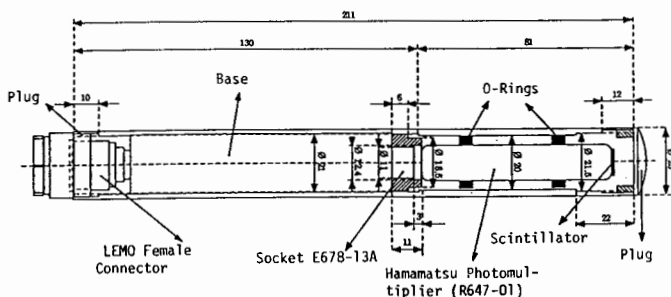


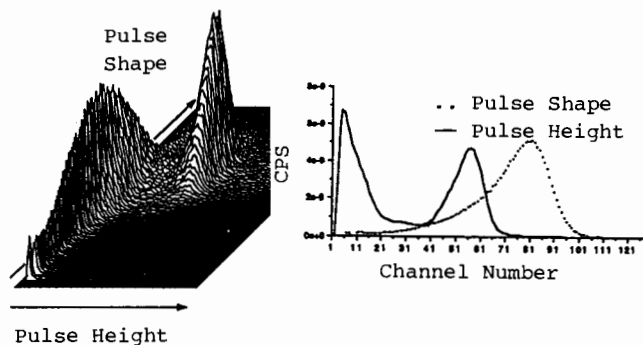
Figure 2: The LGS Detector

### Typical Pulse Height and Shape Spectra

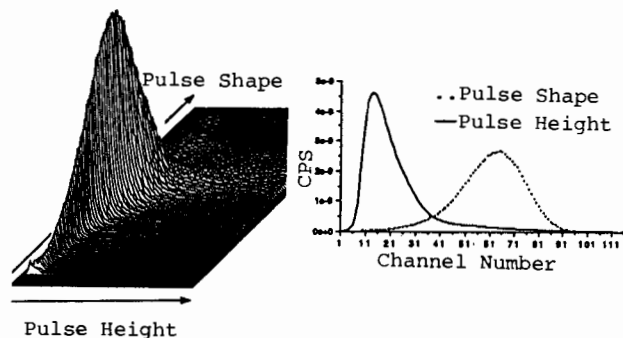
Three-dimensional plots of count rates as a function of pulse height and pulse shape together with their 2-D projections are shown, in Figures 3a and 3b for NE912, where the  $\gamma$  and  ${}^6\text{Li}(n,\alpha)t$  peaks are clearly visible, and in Figures 4a and 4b for NE913, for a soft neutron spectrum location. The measurement duration was much longer (more than twice) for the last LGS. Using  ${}^{22}\text{Na}$  and  ${}^{241}\text{Am}$   $\gamma$  sources, it was confirmed that, for NE912, the right-hand peak comes from the  ${}^6\text{Li}(n,\alpha)t$  reaction.

### Treatment of Data

The 2-D projections of the pulse height spectra (PHS) were considered for data treatment according to the following methods:



Figures 3a + 3b: 3-D and 2-D Spectrum of NE912



Figures 4a + 4b: 3-D and 2-D Spectrum of NE913

(1) LOTUS fitting method: The falling wing of the PHS of NE912 was fitted to the left of the  ${}^6\text{Li}(n,\alpha)t$  peak according to  $y = a x^b$ , where  $a$  and  $b$  are determined by least-squares fitting. A precision of better than 2% was expected. This relationship was then used to extrapolate all through to the right of the peak to obtain the background contribution which was subtracted from the original PHS, giving the  ${}^6\text{Li}(n,\alpha)t$  contribution. The PHS from the NE913 was integrated over the same pulse height range and compared to the previously evaluated value. These two values agreed within 3 to 5%.

(2) JAERI fitting method: Yamaguchi et al.<sup>6</sup> have used NE908 ( ${}^6\text{Li}$ ) and NE906 ( ${}^7\text{Li}$ ) scintillators. The NE906 PHS is first adjusted for the amplifier gain difference vis-a-vis the NE908. Thereafter, a linear transformation is applied on this adjusted PHS for any relative change in the efficiency of the NE908. The PHS's of the two detectors, in the pulse height region lower than the  ${}^6\text{Li}(n,\alpha)t$  peak, is used for the  $\gamma$ -ray background. By a least-squares fitting procedure the two coefficients of the linear transformation are obtained. The background correction evaluated through the linearly transformed PHS of NE906 is then subtracted from that of NE908 to get the  ${}^6\text{Li}(n,\alpha)t$  contribution. The results of both methods agreed within 5%.

### Solid State Nuclear Track Detector Technique

The track that an energetic charged particle leaves in a host medium, when developed by chemical or other etching means, yields information about the particle. The track diameter and length depend, among others, on particle energy, its direction of incidence, its charge and its mass. The etching conditions can be so optimized as to see only certain kinds of particles. In the present experiment, the etching conditions were so optimized as to view both the alpha and the triton tracks under the optical microscope. Three different LiF lithium sources were used. Table 2 lists the relevant data on the source, the detector, and the chemical etchant. One could expect

**Table 2:** Data on the Source, Detector and Etchant

<b>Source</b>	
Material: LiF; Enrichment in ${}^6\text{Li}$ : 95.3%, 0.01%, 7.45% Density: 2.6 g/cm <sup>3</sup> ; Diameter: 2 cm; Thickness: 2 mm	
<b>Detector</b>	
<b>Sensitive layer:</b> Material: LR115 type II (Kodak); Diameter: 17.8 mm; Thickness: 12 $\mu\text{m}$	
<b>Substrate:</b> Material: Polyester; Diameter: 17.8 mm; Thickness: 100 $\mu\text{m}$	
<b>Etchant</b>	
10% NaOH solution at 60 °C during 90 minutes	

that sources (i), (ii) and (iii) would enable to monitor respectively  ${}^6\text{Li}(n,\alpha)t$ ,  ${}^7\text{Li}(n,n'\alpha)t$  and the net contribution from the  ${}^6\text{Li}$  and  ${}^7\text{Li}$  reactions.

**Effective Thickness of the Source ( $x_{\text{eff}}$ ):**

As the LiF source is considerably thicker than the range of  $\alpha$  and  $t$ , it is important to know the fraction of each of them that gets out of the source. The number of  $\alpha$  and  $t$  that enter the detector depends on the neutron spectrum, their respective energies and the distance of their place of generation with respect to the detector. We associate the following  $x_{\text{eff}}$  to each of the average alpha and triton emitted in the  ${}^6\text{Li}$  and  ${}^7\text{Li}$  reactions.

$$\int_0^{\infty} p(x \rightarrow 0) dx$$

$x$  is the distance measured from the surface of the source towards the detector;  $p(x \rightarrow 0)$  is the probability of a particle born between  $x$  and  $x+dx$  to quit the source at  $x=0$  and be intercepted by the detector. A Monte Carlo program, ALPHAMAC, has been written. The spatial profile of the neutron energy spectrum is given as input and is obtained through a 2D discrete-ordinates code DOT3.5<sup>9</sup>. This program samples (1) the place of generation of the charged product inside the source, (2) the energy of the incident neutron, (3) the energy of the product, (4) its range, (5) the probability  $p(x \rightarrow 0)$ . In general,  $x_{\text{eff}}$  would depend on the spatial location of the source-detector pair inside the fusion blanket. Table 3 illustrates the  $x_{\text{eff}}$ 's obtained for a soft neutron spectrum.

**Table 3:**  $x_{\text{eff}}$  For Different Particles and Reactions

Particle	Reaction	$x_{\text{eff}}$
$\alpha$	${}^6\text{Li}(n,\alpha)t$	4.2 $\mu\text{m}$
$\alpha$	${}^7\text{Li}(n,n'\alpha)t$	4.0 $\mu\text{m}$
$t$	${}^6\text{Li}(n,\alpha)t$	26.0 $\mu\text{m}$
$t$	${}^7\text{Li}(n,n'\alpha)t$	25.0 $\mu\text{m}$

**Treatment of Data**

First the track density per unit surface area of the etched detector is obtained. The background of the detector, coming from the sensitive layer of it, should be subtracted. It is found by replacing the LiF source with another detector facing the original one and taking the arithmetic mean of the track densities observed on the two detectors. The precalculated  $x_{\text{eff}}$ 's are used to get the tritium production rates in  ${}^6\text{Li}$  and  ${}^7\text{Li}$ . If  $r_6$  and  $r_7$  respectively represent the

reaction rates per atom and per source neutron of  ${}^6\text{Li}$  and  ${}^7\text{Li}$ , it could be written:

$$T_d = f [ e_6 \cdot r_6 \cdot x_{\text{eff}6} + (1-e_6) \cdot r_7 \cdot x_{\text{eff}7} ] \quad (2)$$

where  $T_d$  is the track density per source neutron;  $f$  is a constant that depends on the source radius, atom density of Li in LiF, the detector radius and the lost tracks;  $x_{\text{eff}6}$  is the sum of  $x_{\text{eff}}$ 's for the alpha and the triton given out by  ${}^6\text{Li}$ ;  $x_{\text{eff}7}$  stands for the  ${}^7\text{Li}$  and  $e_6$  is the enrichment fraction of  ${}^6\text{Li}$  in a given source. It is assumed that  $f$  is the same for all  ${}^6\text{Li}$  enrichments. In the event of the saturation of the track density, the above relationship would breakdown. For a given irradiation time,  $f$  might vary somewhat depending on the track density inside a fusion blanket assembly due to different track density losses. We have chosen two values of  $e_6$ : 0.953 and 0.01. Once  $r_6$  and  $r_7$  are determined, the net tritium production rate per natural Li atom could be estimated as well as the track density for the natural LiF. The latter number could be compared to the measured track density to verify if the determination of the  $r_6$  and the  $r_7$  is acceptably precise. It is to be noted that the need to precalculate the  $x_{\text{eff}}$ 's makes this method somewhat dependent on the neutron transport computation. However, it is well placed to get  $r_7$  which is quite difficult to obtain through other techniques.

**A Benchmark Experiment on a Fusion Blanket**

To test these novel techniques, a benchmark configuration was assembled at our facility. This assembly consists of a 10 cm thick and 103 cm x 117 cm Pb slab followed by a 22 cm thick and 105 cm x 100 cm  $\text{Li}_2\text{CO}_3$  slab. The Pb side of the assembly was at 10 cm from the sealed Haefely 14 MeV neutron generator as is shown in Figure 5:

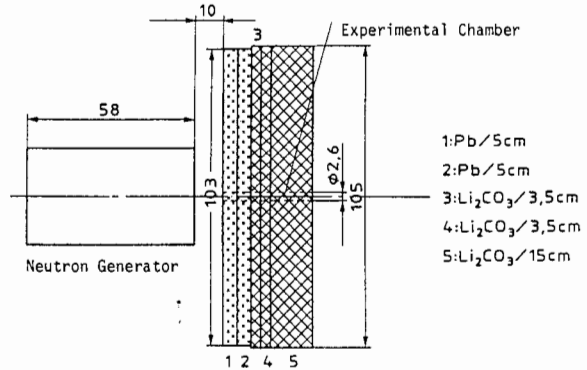


**Figure 5:** Schematic View of the Experimental Set-up

Zr foil detectors are used to normalize the measured tritium production rates per source neutron and to monitor 14 MeV neutrons [ ${}^{90}\text{Zr}(n,2n)$ ]. The detectors were positioned axially at the center of the flat surface of the generator, at the beginning of the Pb slab and every 2.5 cm inside of it. Their measured activities were used for least-squares fitting against the computed values to obtain the source intensity and the standard deviation on it. For the LGS, it was difficult to sufficiently irradiate the Zr foils because of low source intensity. Indium foil [ ${}^{115}\text{In}(n,n')$ ] was used for monitoring purposes and it was established that the error by doing so would be less than 3%.

Five detector locations inside  $\text{Li}_2\text{CO}_3$  were chosen for the LGS measurements (0, 6, 12, 17, 22 cm) and ten for the SSNTD (0, 2.5, 5, 7.5, 10, 12.5, 15, 17.5, 20, 22.5 cm). The demountable experimental tube had the same material composition as the host assembly. The approximate source intensity for the LGS and

SSNTD experiments was respectively  $10^9$  n/s, to avoid the counting-saturation, and  $10^{11}$  n/s. The equivalent irradiation time, for the higher intensity, varied from 5 to 10 minutes.

## Results

### Lithium Glass Scintillation:

A measurement each with NE912 and NE913 were made at a location just behind the  $\text{Li}_2\text{CO}_3$  slab. The  $r_6$  values for the two data treatment methods are :

LOTUS fitting method :  $4.64 \cdot 10^{-29} \pm 4.6\%$

JAERI fitting method :  $4.53 \cdot 10^{-29} \pm 4.3\%$

The  $r_6$  profiles obtained by LGS and SSNTD techniques and normalized to each other near the middle of the  $\text{Li}_2\text{CO}_3$  slab were also compared. Figure 6 shows this comparison:

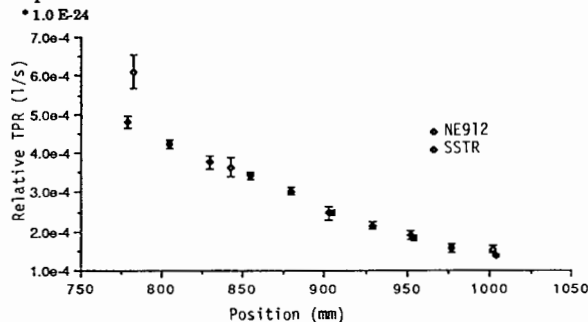


Figure 6:  $r_6$  Profiles Obtained With LGS and SSNTD

It is noticed that except for the first position, the agreement between the two methods is within the statistical error. The reason for the only discrepancy would be saturation of track density for the SSNTD.

2D transport computation was performed with DOT3.5<sup>9</sup> using 46-group EFF-110 cross-section library. The measured value of the absolute LGS efficiency is not known, therefore, the normalization for  $r_6$  measured values is based on a computed result near the middle of the  $\text{Li}_2\text{CO}_3$ . Figure 7 shows these profiles. The basic double differential cross-section data has significant discrepancies for some of the component atoms of the blanket, e.g.,  $^6\text{Li}$ ,  $^7\text{Li}$ , Pb, Al, C and O which could explain the profiles' differences.

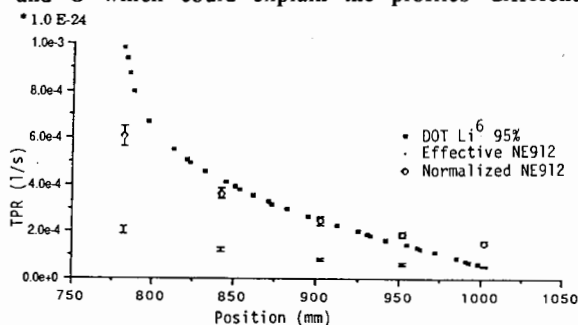


Figure 7:  $r_6$  Profiles with the LGS and 2-D Code

### Solid State Nuclear Track Detection:

The background is found to be very small for  $^6\text{Li}$  enriched and around 10% for  $^7\text{Li}$  enriched  $\text{LiF}$  sources. It is to be remarked that the  $x_{\text{eff}}$  profiles for both the  $\alpha$  and the  $t$  from the  $^6\text{Li}$  reaction are practically flat due to its high Q value of 4.8 MeV. In sharp contrast, the  $x_{\text{eff}}$  profiles for the  $\alpha$  and  $t$  from  $^7\text{Li}(n,n'\alpha)t$  reaction show very large sensitivity to the neutron energy spectrum due to its negative Q value of -2.5 MeV. The  $\alpha$  and  $t$  energies change as a function of the shape of the neutron spectrum above the threshold of 2.8 MeV. Thus, the softening of the

neutron spectrum results in the reduction of the average  $\alpha/t$  energy as well as that of the corresponding  $x_{\text{eff}}$ . The  $x_{\text{eff}}$ 's change by approximately 30-40% across the  $\text{Li}_2\text{CO}_3$ .

The  $r_6$  profiles reflect the same behaviour as for the LGS. Figure 8 shows the  $r_7$  profiles (all the values in the figure are to be multiplied by  $10^{-24}$ )

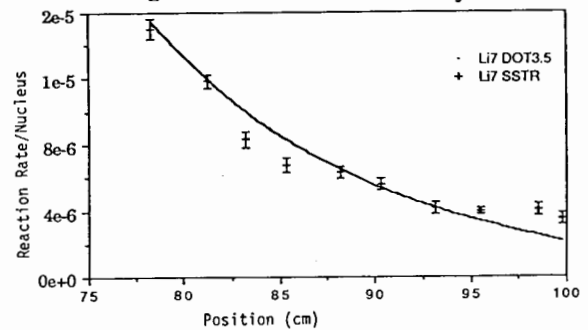


Figure 8:  $r_7$  Profiles Obtained by SSNTD and 2D-Code

It is interesting to see the order of agreement between the two profiles. There are some differences too which might be ascribable to the cross-section data.

## Conclusions

The two techniques of tritium measurement, the LGS and SSNTD, developed and tested at the LOTUS facility, have high sensitivity. As an example, the typical irradiation times, at the equivalent source intensity of  $10^{11}$  n/s for 3% statistical error at a location towards the end of the  $\text{Li}_2\text{CO}_3$ , for the Liquid Scintillation, LGS and SSNTD are respectively 8 hours, 8 minutes and 5-15 minutes. The irradiation time for SSNTD is quite adjustable, depending on the number of fields selected for track-counting and the  $^6\text{Li}$  enrichment of the source. The LGS is ideally suited for online measurement of  $t$  from the  $^6\text{Li}$  reaction while SSNTD can be implemented as a complementary technique for the  $^7\text{Li}$ -reaction, tritium measurements.

## REFERENCES

1. H. Bachmann, U. Fritscher, F. W. Kappler, D. Rusch, H. Werle and H. W. Wiese, Nucl. Sci. Eng., **67**, 74 (1978).
2. R. Herzing, L. Kuypers, P. Cloth, D. Filges, R. Hecker and N. Kirch, Nucl. Sci. Eng., **60**, 169 (1976).
3. H. Maekawa and Y. Seki, J. Nucl. Sci. Tech., **14**, 97 (1977).
4. E. Goldberg, R. L. Barber, N. A. Bonner, C. M. Griffith and D. R. Nethaway, Nucl. Sci. Eng., **94**, 120 (1986).
5. H. Maekawa, K. Tsuda, Y. Ikeda, Y. Oyama, S. Yamaguchi, M. Nakagawa, T. Fukumoto, A. Hasegawa, T. Mori, Y. Seki and T. Nakamura, Fusion Technol., **8**, 1460 (1985).
6. S. Yamaguchi, Y. Oyama, T. Nakamura and H. Maekawa, Nucl. Instr. and Meth., **A254**, 413 (1987).
7. P. B. Price, "Advances in Solid State Nuclear Track Detectors," presented at 13th International Conference on Solid State Nuclear Track Detectors, held in Rome in September, 1985.
8. D.V.S. Ramakrishna, A. Kumar and J.-P. Schneeberger, "Feasibility studies for the estimation of tritium breeding in lithium fusion blankets adopting SSTR techniques," LPR report 141 (October 1986).
9. W. A. Rhoades and F. R. Mynatt, "The DOT III : Two Dimensional Discrete Ordinates Code," Oak Ridge National Laboratory TM-4280 (1979).
10. J. Stepanek, C. E. Higgs, S. Pelloni, J. W. Davidson and D. J. Dudziak, Fusion Technol., **10**, 940 (1986).